Phytopathology Research

RESEARCH

Open Access

Multiomic approaches reveal novel lineage-specific effectors in the potato and tomato early blight pathogen *Alternaria solani*

Jinhui Wang[1,2†], Siyu Xiao[1†], Lijia Zheng[1], Yang Pan[1], Dongmei Zhao[1], Dai Zhang[1], Qian Li[1,2], Jiehua Zhu[1*] and Zhihui Yang[1*]

Abstract

The effectome of the necrotrophic fungal pathogen, *Alternaria solani*, was determined using multiomics. In total, 238 effector candidates were predicted from the *A. solani* genome, and apoplastic effectors constitute most of the total candidate effector proteins (AsCEPs). Comparative genomics revealed two main groups of AsCEPs: lineage-specific and conserved effectors. RNA-Seq analysis revealed that the most highly expressed genes encoding AsCEPs were enriched with lineage-specific forms. Two lineage-specific effector genes, *AsCEP19* and *AsCEP20*, were found to form a 'head-to-head' gene pair located near an AT-rich region on the chromosome. To date, *AsCEP19* and *AsCEP20* have been found only in a few fungal species. Phylogenetic inference revealed that *AsCEP19* and *AsCEP20* were likely acquired by the common ancestor of *A. solani* and *A. tomatophila* via horizontal gene transfer, probably mediated by long terminal repeat retrotransposon. RT-qPCR analysis showed that *AsCEP19* and *AsCEP20* are tightly coexpressed in a host-specific manner and that they are upregulated at advanced stages of *A. solani* infection only in solanaceous hosts. Transient expression of AsCEP19 and AsCEP20 in *Nicotiana benthamiana* plants showed that these effectors could promote *Phytophthora infestans* infection. *AsCEP19* and *AsCEP20* were required for the full virulence of *A. solani* on host potato, because deletion of this gene pair significantly reduced the size of necrotic lesions on potato leaves. Transient expression of AsCEP20 could elicit plant cell death depending on the presence of its signal peptide, indicating that AsCEP20 is a necrosis-inducing apoplastic effector with the mature form localized specifically in chloroplasts. Our work provides a better understanding of the function and evolution of necrotrophic fungal effectors, and helps explain the high aggressiveness of *A. solani* against solanaceous crops.

Keywords: Fungal effector, Early blight, *Alternaria solani*, Omics, Presence-and-absence variation (PAV), Horizontal gene transfer (HGT)

Background

Alternaria solani and *A. tomatophila* (formerly named *A. linariae*) are sister species in phylogeny; both are necrotrophic pathogens that cause early blight in potato (*Solanum tuberosum*) and tomato (*S. lycopersicum*) plants (Woudenberg et al. 2014; Adhikari et al. 2017). In general, species within section *Porri* of the genus *Alternaria* have developed a certain level of host specificity, and are

†Jinhui Wang and Siyu Xiao contributed equally to this work

*Correspondence: zhujiehua@hebau.edu.cn; bdyzh@hebau.edu.cn

[1] College of Plant Protection, Hebei Agricultural University, Baoding 071001, Hebei, China
Full list of author information is available at the end of the article

destructive to their primary host plants (Ozkilinc et al. 2017). For example, *A. solani* and *A. tomatophila* are well adapted to solanaceous crops, such as potato and tomato. *A. solani* varies slightly from *A. tomatophila* in virulence in that *A. solani* is equally aggressive to both potato and tomato plants, but *A. tomatophila* is more aggressive to the latter (Gannibal et al. 2014). Knowledge of the genetic and molecular basis for differences in pathogenicity between *Alternaria* lineages, especially for the high aggressiveness of *A. solani* and *A. tomatophila* on solanaceous crops, is still limited. Previous research on pathogenicity of *Alternaria* species has mainly focused on phytotoxins, plant cell wall-degrading enzymes and melanin (Tsuge et al. 2013; Meena et al. 2017). However, it is still unclear what type of effector proteins are secreted by early blight fungus and how these effectors participate in pathogenicity. Until the present study, no effector has been reported from *A. solani* or *A. tomatophila*.

Pathogenic variation among lineages could be partially explained by the presence-and-absence variation (PAV) of genes. Lineage-specific genes usually play roles in determining virulence, dictating the host range, shaping host specificity, and enabling host jumping (Borah et al. 2018; Fouché et al. 2018; Sánchez-Vallet et al. 2018; de Vries et al. 2020). *Fusarium oxysporum* has diverged into two lineages that infect humans or plants by the acquisition of small chromosomes, which are rich in lineage-specific genes encoding effectors or other virulence factors (Ma et al. 2010; Zhang et al. 2020). Acquisition of lineage-specific genes through horizontal gene transfer (HGT) is an important driving force in fungal evolution. It allows fungal pathogens to acquire new virulence factor genes from other species. The most well-known HGT event between phytopathogenic fungi is related to *ToxA*, which encodes a host-specific toxin (HST) that can interact with the product of the *Tsn1* gene in wheat (Adhikari et al. 2009). Acquisition of *ToxA* by *Pyrenophora tritici-repentis* led to increased virulence and severe tan spot epidemics (Friesen et al. 2006). It has been confirmed that *ToxA* has been subjected to HGT between three different wheat pathogenic fungi, *Parastagonospora nodorum*, *P. tritici-repentis*, and *Bipolaris sorokiniana* (McDonald et al. 2019). HGT is particularly important for those pathogenic fungi that are considered to be strictly asexual, such as *Verticillium dahliae*, *F. oxysporum*, and *A. alternata* (Reinhardt et al. 2021). It has been reported that a lineage-specific fragment encoding virulence factors was horizontally transferred from *F. oxysporum* f. sp. *vasinfectum*, the pathogen causing Fusarium wilt of cotton, to *V. dahliae* strain Vd991, and this HGT event makes strain Vd991 a hypervirulent race on cotton (Chen et al. 2018a, b). HGT of conditionally dispensable chromosomes has been revealed in *Alternaria* species, and therefore different pathogenic lineages can carry extra chromosomes which harbor gene clusters for the biosynthesis of HSTs (Tsuge et al. 2013; Rajarammohan et al. 2019; Wang et al. 2019).

Transposable elements (TEs) are often involved in HGT events, and TE insertions activate repeat-induced point (RIP) mutations in fungal genome to silence the inserted TEs, thereby accumulating G/C to A/T mutations and gradually forming AT-rich regions (Frantzeskakis et al. 2020). The pre-existing AT-rich regions could serve as preferred integration sites for other TEs, followed by various types of mutations, including point mutations, insertions, duplications, recombination, and deletions, while subjected to host or environmental selection pressure, and eventually become lineage-specific regions as shelters for lineage-specific genes (Torres et al. 2020). Typical genomic features of such lineage-specific regions have been reported, such as frequent association with AT-rich repetitive sequences, presence of TE remnants, low gene density, and faster evolution, which are useful characteristics for identifying lineage-specific genes in fungal genomes (Fouché et al. 2018).

Three genome assemblies of *A. solani* (strains BMP0185, HWC168, and NL03003) and one genome assembly of *A. tomatophila* (strain BMP2032) have been published so far (Dang et al. 2015; Wolters et al. 2018; Zhang et al. 2018). The de novo sequence assemblies of *A. solani* BMP0185 and *A. tomatophila* BMP2032 are still highly fragmented (Dang et al. 2015), because the repetitive genomic regions are difficult to assemble using only short reads. The completeness of the genome sequence of *A. solani* HWC168 is better, because it was assembled using Illumina paired-end and mate-pair reads (Zhang et al. 2018). The genome sequence of *A. solani* NL03003 was assembled using long reads generated from PacBio SMRT sequencing, and NL03003 is the only completely assembled *A. solani* genome reported to date (Wolters et al. 2018). A contiguous genome assembly is essential, when the aim is to identify novel effectors or other virulence factors, which are often associated with lineage-specific genomic regions. Nevertheless, analysis of these complete or draft genomes provide insights into the biology of early blight pathogens, and these data are valuable genomic resources for comparative genomic studies.

Here, effector candidates were predicted from the *A. solani* genome, and genome comparisons were preformed to assess the evolutionary conservation of the effector genes in *Alternaria* species. RNA-Seq data were used to identify the effector genes that were highly expressed in planta. A series of assays, including phylogenetic inferences, gene expression analysis, *Agrobacterium*-mediated transient expression, and gene knockout

were performed to reveal the roles of lineage-specific effectors in the virulence of this early blight pathogen.

Results

Effector candidates in *A. solani*

The genome of *A. solani* HWC168 was predicted to possess 11,951 protein-coding genes (Additional file 1: Table S1), of which 238 (1.99%) were considered to be candidate effector proteins (CEPs) (Additional file 1: Table S2). Of the *A. solani* CEPs (AsCEPs), 157 (65.97%) and 28 (11.76%) were classified as apoplastic and cytoplasmic effectors, respectively, and 53 (22.27%) could be dual localized effectors (Fig. 1a and Additional file 1: Table S2). Obviously the apoplastic effectors constitute the major group of the total effector (p-value 8.38e^{-7}, χ^2 test). Based on the RNA-Seq data of *A. solani* (Additional file 1: Table S3), 209/238 (87.8%) AsCEP genes were defined as effector genes expressed in planta but with different expression levels (Additional file 1: Table S2): 10 AsCEP genes were expressed at high levels in potato leaves and ranked within the top 200 among all protein-coding genes, while 111 and 88 AsCEP genes had moderate and low expression levels, respectively (Fig. 1b). Conserved long range synteny was observed between the genomes of strains HWC168 and NL03003 (Additional file 2: Figure S1); furthermore, all AsCEP genes predicted in strain HWC168 have homologs in strain NL03003 and exhibit high collinearity (Fig. 1c), indicating a high level of conservation in gene content and genome structure.

Conservation of AsCEP genes within the genus *Alternaria*

Among the 29 *Alternaria* species whose genomes have been sequenced (Additional file 1: Table S4), our PAV analysis of the genes encoding AsCEPs displayed 'two-peaks' (Fig. 2a). The first peak represents a cluster of 30 (12.6%) AsCEP genes that were only identified in *A. solani* or were also found in a sister species, suggesting that their functions might be associated with pathogenic traits within a very narrow lineage. The second peak consists of 101 (42.4%) genes encoding AsCEPs that were commonly found in at least 27 (90%) *Alternaria* species and represent a cluster of conserved effectors in the genus. Interestingly, the most highly expressed AsCEP genes were enriched with lineage-specific effectors (p-value 3.68e^{-3}, Fisher's exact test), suggesting that *A. solani* has evolved a unique effector arsenal that appears to rely heavily on lineage-specific effectors (Fig. 2a and Additional file 1: Table S2). Of the

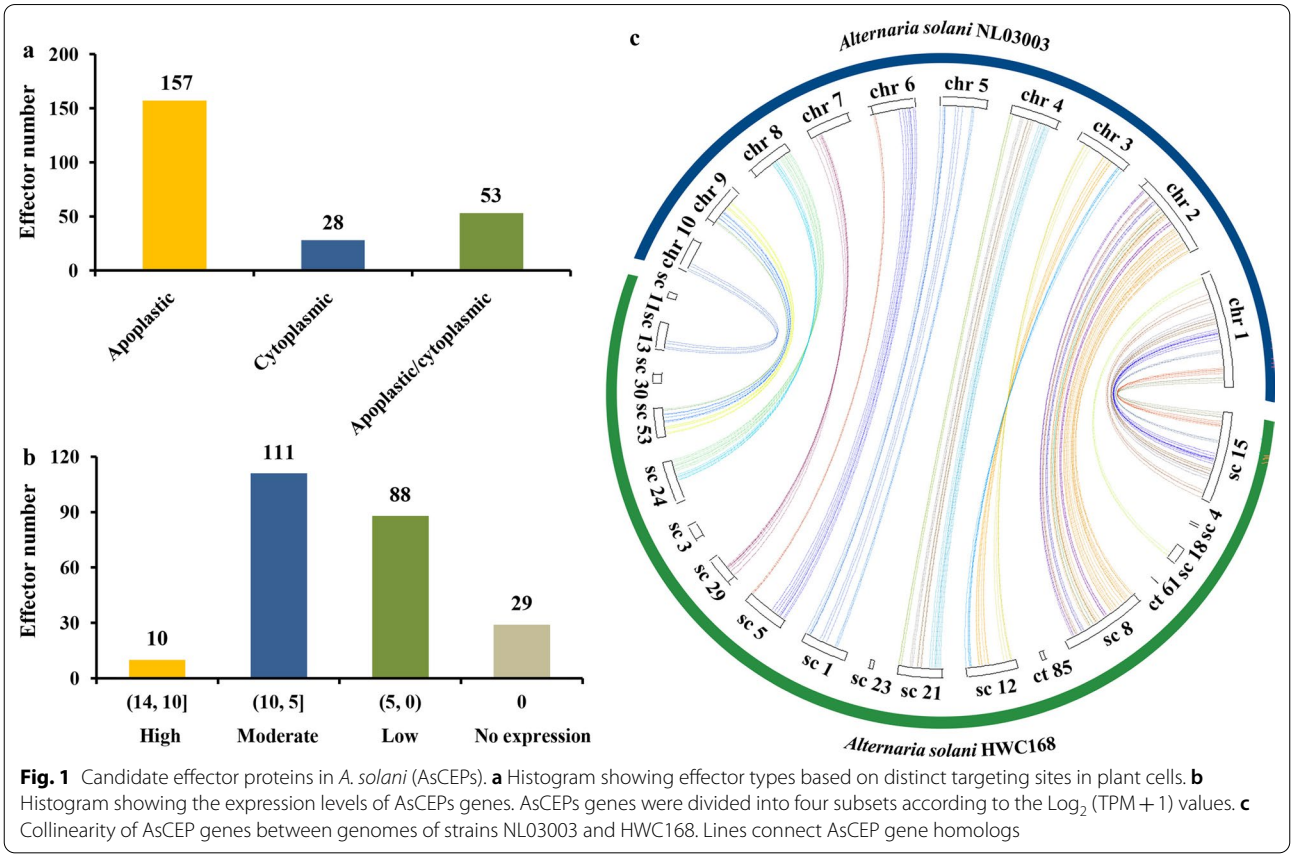

Fig. 1 Candidate effector proteins in *A. solani* (AsCEPs). **a** Histogram showing effector types based on distinct targeting sites in plant cells. **b** Histogram showing the expression levels of AsCEPs genes. AsCEPs genes were divided into four subsets according to the Log_2 (TPM + 1) values. **c** Collinearity of AsCEP genes between genomes of strains NL03003 and HWC168. Lines connect AsCEP gene homologs

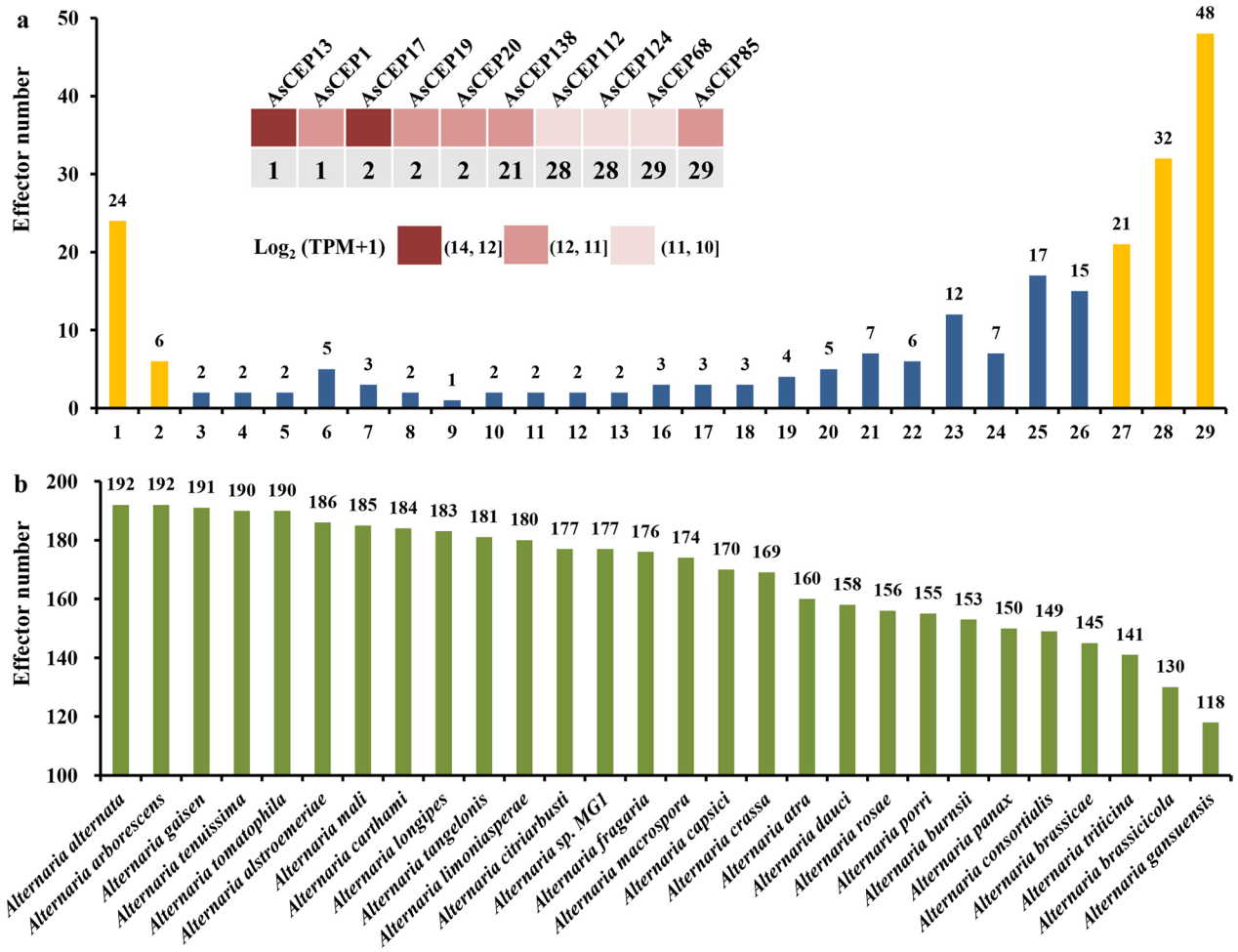

Fig. 2 Presence-and-absence variation (PAV) of AsCEPs genes in *Alternaria* species. **a** Histogram showing the counts of AsCEPs genes that were found in one to twenty-nine (X-axis) *Alternaria* species, and heatmap showing the conservation of the most highly expressed AsCEPs genes. Yellow columns represent effector genes found in more than 26 or less than three *Alternaria* species. The number indicated on each column represents the count of AsCEP genes. Colors in heatmap represent the Log_2 (TPM + 1) values, and the numbers in grey boxes represent the number of *Alternaria* species in which each gene was found. **b** The number of AsCEPs genes that have homologs in other *Alternaria* species

lineage-specific AsCEP genes that are highly expressed, *AsCEP17* encodes a hypothetical protein that did not return any hit in UniProtKB. *AsCEP1* and *AsCEP13*, *AsCEP19* and *AsCEP20* encode hypothetical proteins which have homologs in *Cochliobolus heterostrophus* and *Corynespora cassiicola*, respectively. Of the conserved and highly expressed AsCEP genes, *AsCEP138* encodes a virulence factor, hydrophobin, while other genes encode hypothetical proteins with unknown function. *A. alternata*, *A. arborescens*, *A. gaisen*, *A. tomatophila*, and *A. tenuissima* share at least 190 (79.8%) effector genes with *A. solani*, while *A. gansuensis* has the fewest effector genes (118) in common with *A. solani* (Fig. 2b).

Novel lineage-specific AsCEP genes

Of the lineage-specific AsCEP genes showing high levels of expression, *AsCEP19* and *AsCEP20* lie adjacent to each other, constituting a bidirectional (head-to-head, H2H) gene pair which is located within a small GC-equilibrated region (15 kb) on chromosome 3 (CP022026.1.3) of strain NL03003 (Fig. 3). The small GC-equilibrated region is flanked by two AT-rich regions, which are located between positions 199,848 and 242,843 (43 kb) and positions 257,850 and 284,655 (26.8 kb) on this chromosome, respectively (Fig. 3). The distance between the 3' end of *AsCEP19* and nearby AT-rich region is only 1,012 bp (Additional file 1: Table S5). Two similar (94% identity) gypsy-family long terminal repeat (LTR) elements were found in the

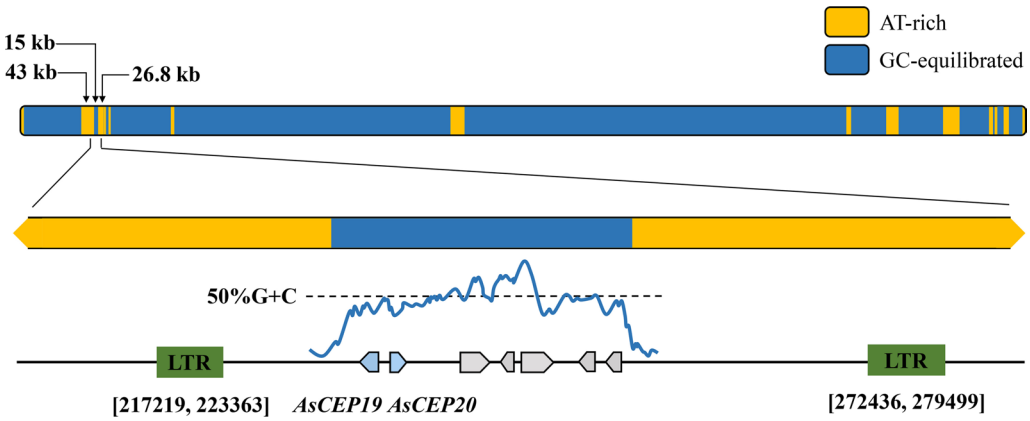

Fig. 3 Schematic diagram of the *AsCEP19* and *AsCEP20* loci on chromosome. The GC-equilibrated and AT-rich regions in the *A. solani* strain NL03003 chromosome 3 (CP022026.1.3) were shown in colors. Protein-coding genes and long terminal repeat (LTR) elements were shown as arrows and rectangles in colors, respectively. The GC content was shown along the selected region. In the 5′ to 3′ orientation, *AsCEP19* is located between positions 244,287 and 243,852, and *AsCEP20* is located between 246,214 and 246,637

flanking AT-rich regions, which are located from base pairs 217,219 to 223,363 and from 272,436 to 279,499, respectively. Within the *Alternaria* genus, *AsCEP19* and *AsCEP20* only present in *A. solani* and sister species *A. tomatophila*, which also cause early blight of potato and tomato.

Homologs of AsCEP19 and AsCEP20

Both AsCEP19 and AsCEP20 are small secreted proteins that are rich in cysteine (9/99 and 8/102, respectively) and are most likely to be homologs of the putative small secreted proteins, which have been reported in the *C. cassiicola* strain Philippines (CCP), a fungal pathogen causing leaf fall disease on rubber trees (Lopez et al. 2018). The CCP genome contains two genes (*BS50DRAFT_638061* and *BS50DRAFT_64582*) homologous to *AsCEP19* and one gene (*BS50DRAFT_627105*) homologous to *AsCEP20* (Fig. 4a). In contrast to *AsCEP19* and *AsCEP20* that form an H2H gene pair, the CCP homologs are located on different scaffolds. Genes homologous to *AsCEP19* have only been found in CCP so far, but genes homologous to *AsCEP20* have also been discovered in some *Colletotrichum* species (Fig. 4a). AsCEP19 has no known domain, but AsCEP20 contains a fungal calcium-binding domain PF12192 (HMMER search e-value $1.5e^{-9}$), suggesting that AsCEP20 is a distant homolog of CBP1, a well-known virulence factor identified in the human fungal pathogen *Histoplasma capsulatum* (Sebghati et al. 2000). AsCEP20 also contains the six conserved cysteine residues, a characteristic of CBP1 (Batanghari et al. 1998). In addition, AsCEP20 and its homologs found in other phytopathogens contain two more cysteine residues (Additional file 2: Figure S2).

Putative origins of *AsCEP19* and *AsCEP20*

The gene trees (Fig. 4a) and species tree (Fig. 4b) indicates that *AsCEP19* and *AsCEP20* do not have a vertical descent origin. Within the *Alternaria* genus, *AsCEP19* and *AsCEP20* are only present in *A. solani* and sister species *A. tomatophilia*, and their homologs have been found in very few fungal species outside this genus (Fig. 4a). It is still unclear whether *AsCEP19* and *AsCEP20* arose through HGT or have de novo origins as 'orphan' genes. Although the CCP genome harbors homologs of *AsCEP19* and *AsCEP20*, these homologs were weakly expressed at non-infection (spore suspension) or infection (in planta) stages. The total RNA-Seq read counts of the *AsCEP19* homologs, *BS50DRAFT_638061* and *BS50DRAFT_64582*, were all less than 30 in all the RNA-Seq samples, and no significant upregulation was detected in planta (Fig. 4a). Only six read pairs were mapped to the *AsCEP20* homolog *BS50DRAFT_627105* in all samples, suggesting its insignificant role in CCP. Low expressions of the CCP homologs were similar, as reported (Lopez et al. 2018). However, as a remote homolog of *AsCEP20*, the *CBP1* gene is actively expressed (Log2 fold change > 9, adjusted p-value < 0.001) in the yeast phase (parasitic form) of *H. capsulatum*; this result is consistent with previous work (Gilmore et al. 2015).

Expression profiles of *AsCEP19* and *AsCEP20* in solanaceous and non-solanaceous hosts

Expression levels of *AsCEP19* and *AsCEP20* were significantly upregulated in the leaves of host plants upon *A. solani* infection (Fig. 5) when compared with those in *A. solani* grown on potato dextrose agar (PDA) plates.

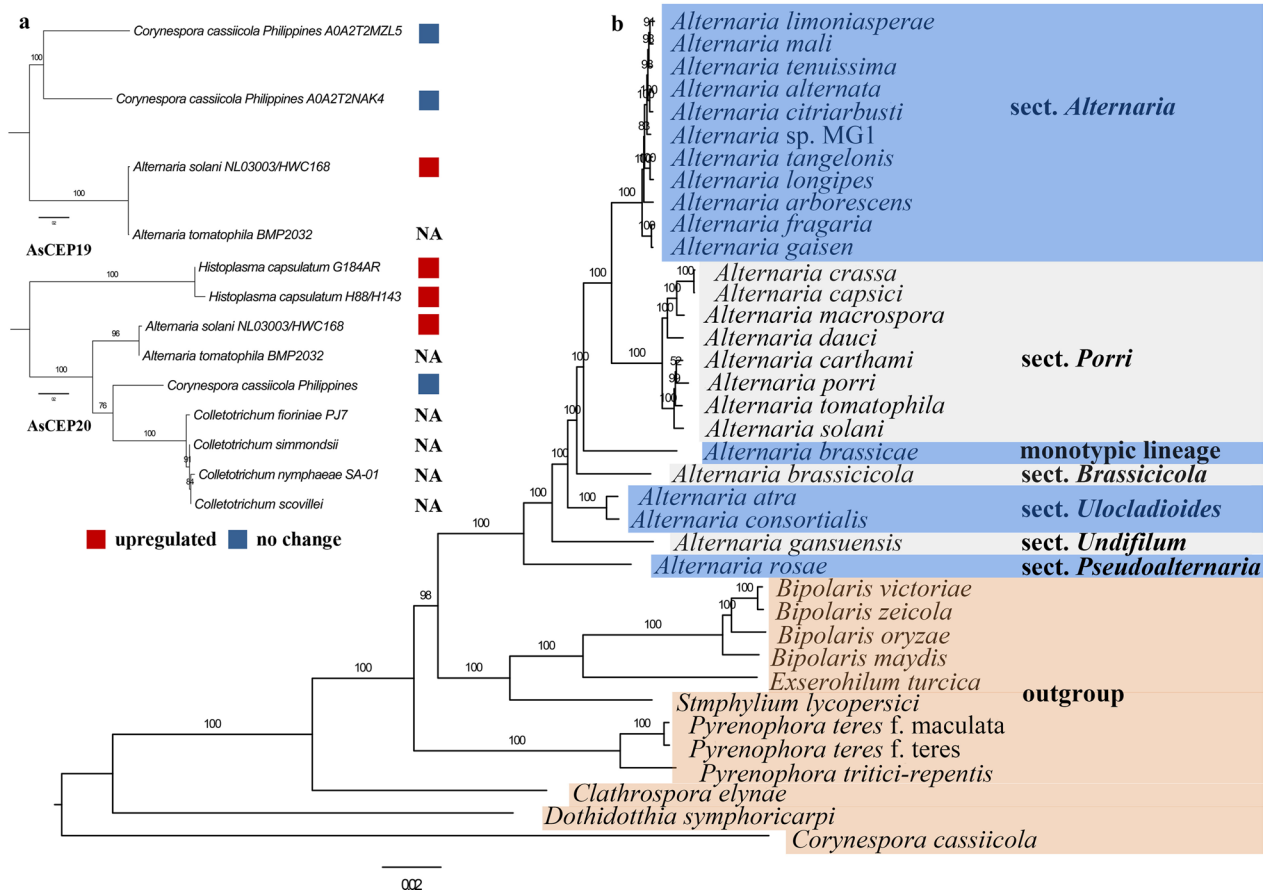

Fig. 4 Gene trees of AsCEP19 and AsCEP20 and species tree of the genus *Alternaria*. The best amino acid substitute models were determined using ProtTest. Maximum-likelihood trees were constructed using RAxML. **a** Phylogenetic trees constructed according to amino acid sequences of AsCEP19, AsCEP20 and their homologous proteins. The numbers shown next to the branches indicate the percentage of bootstrap support values (1000 replicates). The branch lengths indicate the evolutionary distance as the number of base substitutions per site. The rectangular boxes represent the changes in the gene expression during fungal infection. NA, data not available; **b** Phylogenetic tree constructed according to the alignments of 1,216 single-cpoy protein-coding genes from 37 fungal genome datasets. The 1,216 orthogroups were aligned using MAFFT, and these multiple alignments were trimmed and concatenated into a super-matrix

Interestingly, this H2H gene pair showed positive correlation in expression under all conditions, with the 95% confidence interval of Pearson's correlation coefficient of 0.82–0.98 (p-value 1.06e^{-6}). *AsCEP19* and *AsCEP20* were significantly upregulated at 24, 48, and 72 h post-inoculation (hpi) in potato leaves (Fig. 5a), furthermore, high expression levels were also observed in the other two solanaceous hosts, tomato (*Solanum lycopersicum*) (Fig. 5b) and chili pepper (*Capsicum annuum*) (Fig. 5c), where *AsCEP19* and *AsCEP20* were consistently expressed at 48, 72, and 96 hpi, indicating that both of these effector genes play important roles in the interactions between *A. solani* and solanaceous hosts. In contrast, *AsCEP19* and *AsCEP20* showed low expression levels in the non-solanaceous host, *Arabidopsis thaliana* (Fig. 5d), where the average Ct values of the two genes were greater than 34.59 and 35.34, respectively. The different expression patterns of *AsCEP19* and *AsCEP20* in solanaceous and non-solanaceous hosts suggest that the expression of this gene pair is controlled strictly in a host-specific manner.

Transient expression of AsCEP19 and AsCEP20 in *N. benthamiana*

To better understand the roles of AsCEP19 and AsCEP20 in pathogenicity, the two effector genes were transiently expressed in *N. benthamiana* leaves via agroinfiltration. Only the full length (FL) form of AsCEP20 was able to trigger plant cell death in *N. benthamiana*, but not the signal peptide-deleted (ΔSP) form, indicating that the SP is essential for AsCEP20 to induce plant cell death (Fig. 6a). Plant cell death induced by AsCEP20^{FL} was also observed in tomato leaves (Fig. 6b). Neither the FL nor the ΔSP forms of these two effectors could suppress

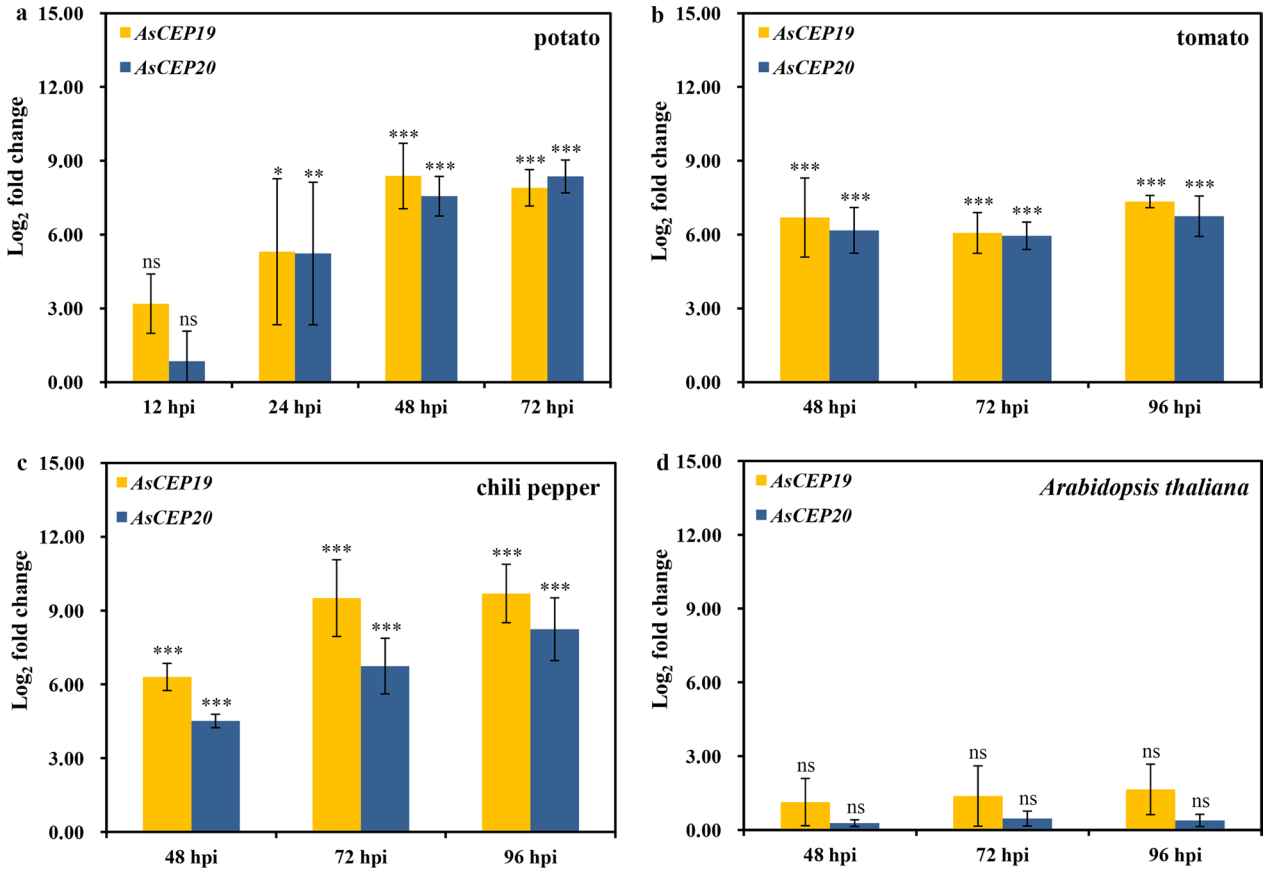

Fig. 5 RT-qPCR analysis of *AsCEP19* and *AsCEP20* expression during *A. solani* infection of potato (**a**), tomato (**b**), chili pepper (**c**), and *Arabidopsis thaliana* (**d**) leaves. The expression levels of *AsCEP19* and *AsCEP20* in planta at different time points after inoculation were compared with those during mycelial growth of *A. solani* on PDA. Actin gene (*ACTB*) of *A. solani* was used as reference gene. Error bars represents means ± SD from five biological replicates. Two-tailed Student's *t* tests, $^{*}P < 0.05$, $^{**}P < 0.01$, and $^{***}P < 0.001$, ns means not significant

INF1-triggered plant cell death in *N. benthamiana* (Additional file 2: Figure S3). Transient expression of AsCEP19 and AsCEP20 in *N. benthamiana* could promote *P. infestans* infection. No necrotic lesions were observed on the zone agroinfiltrated with the effector genes (*AsCEP19* or *AsCEP20*) for 48 h. After inoculation with *P. infestans*, necrosis was observed at the inoculation site, and the necrotic zone enlarged gradually but not exceeded the agroinfiltration zone. The size of necrotic lesions on leaf tissue infiltrated with the $AsCEP19^{FL}$ or $AsCEP20^{FL}$ construct was significantly larger than that inoculated with the *GFP* control (Fig. 6c). Although $AsCEP20^{FL}$ induces plant cell death, which suggests that it can act as a necrotrophic effector in apoplastic space, we cannot exclude the possibility that AsCEP20 might have other functions in the cytoplasm. To investigate whether AsCEP19 and AsCEP20 have a potential targeting site within plant cells, AsCEP19-YFP and AsCEP20-YFP fusion proteins were transiently expressed in *N. benthamiana* leaves via agroinfiltration. AsCEP19-YFP was observed in multiple subcellular compartments including the plasma membrane, nucleus, and cytoplasm, which resembled the free GFP control (Fig. 7). Interestingly, AsCEP20-YFP has a specific subcellular localization that was only found in the chloroplasts, suggesting that these organelles might be potential targets.

AsCEP19 and AsCEP20 contribute to the full virulence of *A. solani*

Gel electrophoresis of the PCR amplicons (Additional file 2: Figure S4) and their sequencing results (Additional file 1: Table S6) confirmed that the entire region spanning the H2H gene pair (*AsCEP19* and *AsCEP20*) in *A. solani* HWC168 had been replaced by the hygromycin phosphotransferase gene (*HPH*). The deletion of *AsCEP19* and *AsCEP20* (Δ*AsCEP19*+*AsCEP20*) from *A. solani* HWC168 led to reduced virulence on potato leaves (Fig. 8). The necrotic lesion (Fig. 8a) caused by the gene deletion mutant Δ*AsCEP19*+*AsCEP20* (1.81 ± 1.16 mm) was much smaller than that of the

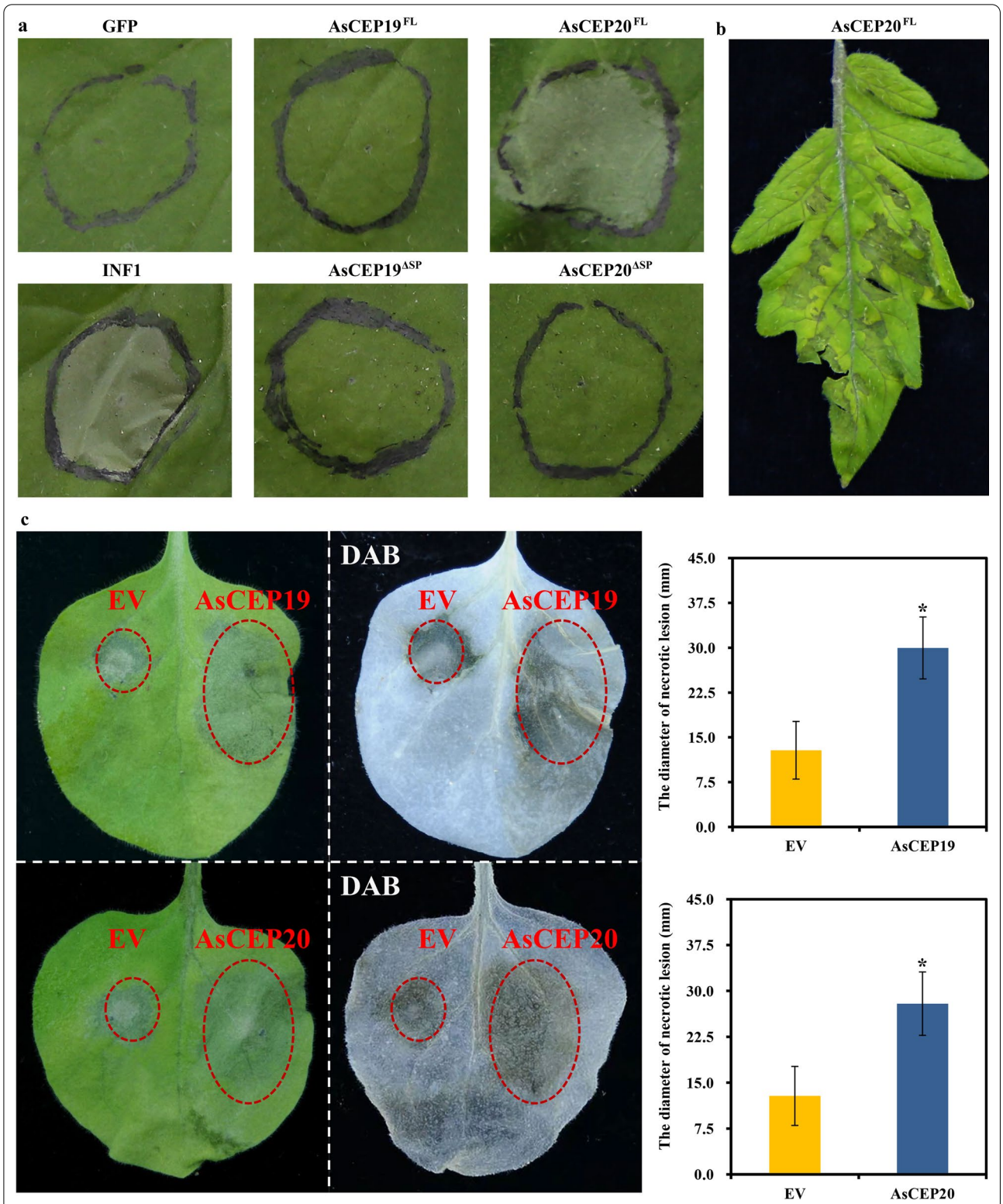

Fig. 6 Transient expression of AsCEP19 and AsCEP20 in *N. benthamiana* and tomato leaves. **a** The full-length (FL) AsCEP20 (AsCEP20^{FL}) triggered obvious necrotic lesion at seven days post-infiltration. The GFP and INF1 plasmid constructs were infiltrated as negative and necrosis control, respectively. **b** AsCEP20^{FL} elicited plant cell death in tomato leaves. **c** AsCEP19^{FL} and AsCEP20^{FL} promoted *P. infestans* infection in *N. benthamiana*. AsCEP19^{FL}, AsCEP20^{FL}, and GFP (empty vector) were individually agroinfiltrated into leaves for 48 h, and then the infiltrated leaves were detached from plants and inoculated with 10 µL zoospore suspension (5×10^4 zoospores/mL) of *P. infestans*. At 5 days post-inoculation (dpi), lesion size was measured, and the leaves were stained with DAB (Two-tailed Student's *t* test, * $P < 0.05$, ± SD, n = 6)

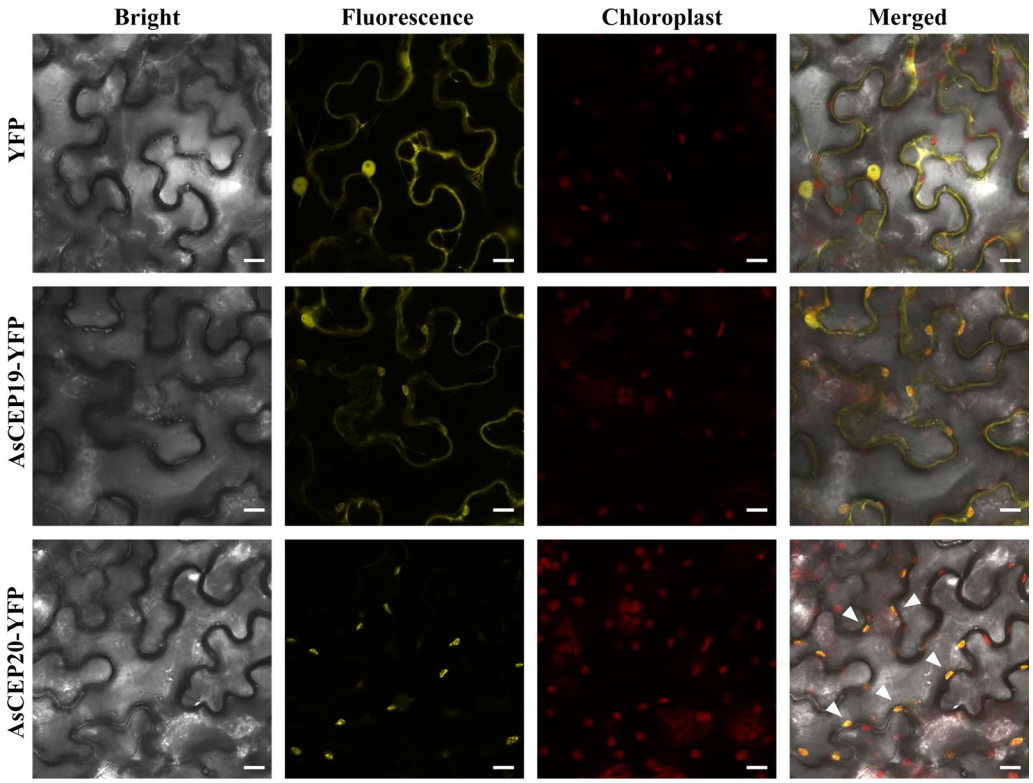

Fig. 7 Subcellular localization of AsCEP19 and AsCEP20 in *N. benthamiana* leaves. *N. benthamiana* leaves were infiltrated with *A. tumefaciens* GV3101 carrying AsCEP19-YFP, AsCEP20-YFP, or YFP plasmid constructs. Upper panels show the localization of free YFP as a control. The middle panels and bottom panels show the localization of AsCEP19-YFP and AsCEP20-YFP, respectively (arrows point to the chloroplasts). Bars, 10 μm

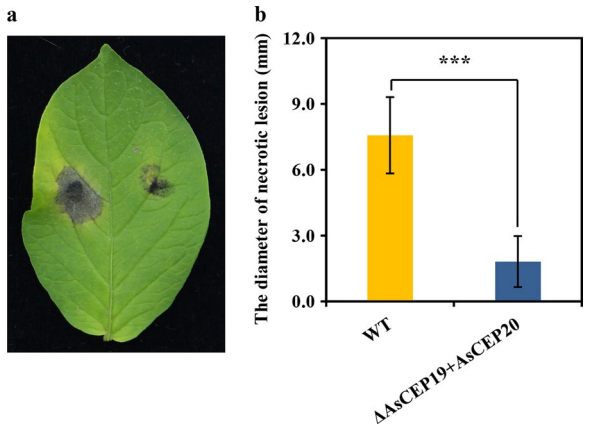

Fig. 8 Variation in virulence between the gene pair (*AsCEP19* and *AsCEP20*)-knockout mutant and wild-type of *A. solani* on potato leaves. **a** Detached potato leaves inoculated with conidial suspensions of the wild-type strain (left) and the Δ*AsCEP19*+*AsCEP20* mutant (right). The sizes of necrotic lesions were measured at 5 dpi. **b** The average size of necrotic lesions caused by the Δ*AsCEP19*+*AsCEP20* mutant and the wild-type strain. Error bars indicate the standard deviation of the mean, and asterisks indicate statistical significance determined by paired *t*-test ($t=16.16$, p-value $=2.5e^{-11}$, df $=16$, n $=17$), with three (***) $P<0.001$

wild-type (7.57 ± 1.74 mm), the p-value of a paired t-test ($t=16.16$) was $2.5e^{-11}$ (Fig. 8b). Thus, this H2H gene pair contributes significantly to the full virulence of *A. solani* on host potato plants.

Discussion

In this study, effector candidates were identified in *A. solani* using a multiomics approach. Most of the AsCEPs were predicted to be apoplastic effectors (Fig. 1a), consistent with the lifestyle of *A. solani* in that the necrotrophic fungal genome is enriched with apoplastic effectors (Lo Presti et al. 2015; Sperschneider and Dodds 2022). On the whole, most of the AsCEP genes appear to be conserved and their homologs were also found in many other closely related species (Fig. 2a, b), however, based on the actual expression levels of AsCEP genes in planta, it was evident that *A. solani* largely relies on few lineage-specific effectors (Figs. 1b and 2a), but so far, their functions remain unclear. Of the lineage-specific AsCEP genes showing high expression levels, *AsCEP19* and *AsCEP20* appear to have been acquired by the common ancestor of *A. solani* and *A. tomatophila* via HGT based

on phylogenetic analysis and characteristics of gene loci, however, given the limited presence of *AsCEP19* and *AsCEP20* in the fungal kingdom, other possibilities, such as de novo gene birth, cannot be excluded (Figs. 3 and 4).

Both *AsCEP19* and *AsCEP20* have a high content of cysteine residues that might be involved in disulfide bond formation to enhance stability in a protease-rich apoplast environment (Wang et al. 2020). Furthermore, it is known that lineage-specific effector genes preferentially associate with AT-rich and gene-poor chromosomal regions (Testa et al. 2016), and *AsCEP19* and *AsCEP20* are no exceptions (Fig. 3). The presence of LTRs in nearby AT-rich regions suggests that this putative HGT event was very likely mediated by an LTR retrotransposon. However, we still lack conclusive evidence of the donor organism of *AsCEP19* and *AsCEP20*. At present, both homologs of *AsCEP19* and *AsCEP20* are only known from the necrotrophic fungus *C. cassiicola* strain Philippines (CCP), a highly virulent isolate from the rubber tree (Lopez et al. 2018). In contrast to *AsCEP19* and *AsCEP20* organized in an H2H arrangement near AT-rich regions, the CCP homologs are located in conserved core genomic regions but on different scaffolds. None of the CCP homologs were truly expressed in host plants (the rubber tree), so it is possible that these two effectors were previously required for pathogenicity but no longer needed for infection of rubber tree and have become silenced. Avirulence (*Avr*) gene silencing has been shown to be an efficient mechanism for *Phytophthora* pathogens to evade effector-triggered immunity (Dong and Ma 2021). AsCEP20 contains a fungal calcium-binding domain, PF12192, which was originally identified in CBP1, a critical virulence factor for *H. capsulatum* known to cause histoplasmosis in human (Sebghati et al. 2000). AsCEP20 shares conserved cysteine residues involved in disulfide bond formation in CBP1 (Beck et al. 2008). Although the sequence similarity suggests that AsCEP20 is a distant homolog of CBP1, more studies need to be conducted to determine whether it still retains the function of CBP1: calcium binding and uptake.

Genes in H2H pairs are often coexpressed and functionally related (Chen et al. 2010). Overall, the H2H gene pair we identified here (*AsCEP19* and *AsCEP20*) was highly expressed in planta but not in vitro. A previous study showed that *A. solani* conidia germination and germ tube elongation were observed at 12 hpi; penetration was first observed at 24 hpi and increased at 36 hpi (Dita et al. 2007). The expression level of the H2H gene pair was only slightly upregulated at 12 hpi but this was not significant (Fig. 5a). Thus, AsCEP19 and AsCEP20 do not belong to the first wave of secreted effectors, therefore their functions are probably insignificant in the initial colonization period when attached conidia germinate and grow on the potato leaf surface (0–12 hpi). However, the expression level of the H2H pair was upregulated markedly at 12–24 hpi, and remained high (Log2 fold change > 7) at 48 and 72 hpi. This result indicates that these two effectors play important roles at advanced stages, including penetration and hyphae spread subepidermally in plant leaves. Furthermore, the high expressions of *AsCEP19* and *AsCEP20* in other solanaceous hosts (Fig. 5b, c), chili pepper and tomato, were also confirmed, but not in the non-solanaceous host *A. thaliana* (Fig. 5d). Taken together, this coexpressed H2H gene pair is strictly regulated and involved in the interaction of *A. solani* and solanaceous hosts, and probably plays key roles to facilitate *A. solani* infection at post-penetration stages.

Transient expression in *N. benthamiana* showed that both AsCEP19 and AsCEP20 can promote the infection of *P. infestans*, indicating their roles in virulence (Fig. 6c). Their function in fungal virulence was further determined by comparing the pathogenicity between the gene deletion mutant and wild-type strain (Fig. 8). Our results confirmed that the H2H gene pair was required for the full virulence of *A. solani* towards host potato plants. Based on the phenotypes incurred by transient expression of AsCEP20 in *N. benthamiana* and tomato, AsCEP20 is probably a necrotrophic effector that requires its SP to induce plant cell death (Fig. 6a, b). Similar findings have also been reported in *Rhizoctonia solani* (Wei et al. 2020) and *F. graminearum* (Yang et al. 2021). AsCEP20 was predicted to be an apoplastic effector, but surprisingly, AsCEP20$^{\Delta SP}$ was specifically localized in chloroplasts (Fig. 7). The chloroplast is prime target of effector proteins since it is the major source of reactive oxygen species generation and a key component of early immune responses (de Torres Zabala et al. 2015). We cannot rule out the possibility that AsCEP20 might have a dual functionality. It is likely that AsCEP20 is secreted into the apoplastic space and subsequently re-enters the host cell cytoplasm, as similar traits have been reported in the *Zymoseptoria tritici* effector Zt6 (Kettles et al. 2018). Further studies are needed to uncover how AsCEP20 localizes to chloroplasts.

Effector genes acquired via HGT commonly play important roles in the evolution of fungal pathogens, by providing novel genetic materials involved in pathogenicity or associated with lineage specific niche adaptation (Fouché et al. 2018; Frantzeskakis et al. 2020). In contrast to core effector genes that are relatively conserved across fungal species, the effector genes acquired via HGT by *A. solani* might favor its host's adaptation to solanaceous hosts. HGT is a significant source of genetic variability, and is particularly important for those fungal species that

lack sexual reproduction (Wang et al. 2019; Reinhardt et al. 2021), such as *A. solani*.

Conclusions

In this study, 238 effector genes were predicted from the *A. solani* genome. Comparative genomics and transcriptomics analysis revealed that *A. solani* has developed a sophisticated effector arsenal and relies on certain lineage-specific effectors to interact with solanaceous hosts. A pair of lineage-specific effector genes, *AsCEP19* and *AsCEP20,* was identified and they seem to have arisen by HGT. Upregulation and coexpression of *AsCEP19* and *AsCEP20* during *A. solani* infection suggests their important roles in promoting the infection of solanaceous hosts and they might be functionally related. Deletion of this gene pair confirmed that *AsCEP19* and *AsCEP20* were required for the full virulence of *A. solani* towards host potato plants. Transient expression of AsCEP19 and AsCEP20 can facilitate the infection of *P. infestans* in *N. benthamiana*. AsCEP20^{FL} elicits plant cell death indicating that it is a necrotrophic effector, and AsCEP20$^{\Delta SP}$ can specifically localize to chloroplasts.

Methods

Computational prediction of effector genes in *A. solani*

First, gene prediction was performed on the genome of *A. solani* HWC168 (GCA_002837235.1) using BRAKER2 v2.1.6 (Hoff et al. 2015). The proteome of closely related species *A. alternata* SRC1lrK2f (GCA_001642055.1) was used as a reference genome. In addition, RNA-Seq data (PRJNA574559) from our previous study were also used to improve gene prediction (Additional file 1: Table S3). The RNA-Seq datasets were generated from potato leaves that were sprayed with spores of *A. solani* HWC168 and subsequently detached at 48 hpi. The transcriptome of *A. solani* HWC168 was assembled de novo from RNA-Seq data using Trinity v2.12.0 (Grabherr et al. 2011); then alternative splicing variations were determined using PASA v2.4.1 (Haas et al. 2003). Finally, a consensus gene structure of *A. solani* HWC168 was generated by EVidenceModeler v1.1.1 (Haas et al. 2008) using evidence from BRAKER2 gene prediction and de novo transcripts.

Genes encoding CEPs were identified from the protein-coding genes of *A. solani* HWC168. A bioinformatics pipeline was established, which was modified from the general pipeline for prediction of candidate secreted effector proteins described in a previous review (Dalio et al. 2018). The pipeline consists of four steps and is executed in the following order: i) prediction of putative secreted proteins using SignalP v6.0 (Teufel et al. 2022) and WoLF PSORT (Horton et al. 2007); ii) removal of membrane proteins with TMHMM v2.0 (Krogh et al. 2001); iii) removal of glycosylphosphatidylinositol (GPI) anchors using NetGPI (Gíslason et al. 2021); and iv) identification of CEPs by EffectorP v3.0 (Sperschneider and Dodds 2022). These AsCEPs were functionally annotated by BLASTp against the UniProtKB database, and protein domains were identified by SMART searching (e-values < $1e^{-5}$).

Synteny conservation between *A. solani* strains

Intraspecific variation in *A. solani* is still unknown, *A. solani* strains from different origins might possess dramatic structural variations in local genome architecture, especially in the regions where the effector genes are located. Therefore, long-range synteny between the genome assemblies of *A. solani* strains was analyzed using MCScanX (Wang et al. 2012), and local gene collinearity between two strains were further examined. Although three *A. solani* strains are available in NCBI and JGI MycoCosm, unfortunately the genome assembly of strain BMP0185 (JGI) consists of more than 2,000 contigs which was too fragmented to be included in the analysis. Therefore, synteny conservation between the genomes of strains NL03003 and HWC168 was evaluated.

Identification of PAV of AsCEP genes in *Alternaria* species

Genome sequences of *Alternaria* species available from GenBank and JGI MycoCosm (as of March 2022) were used to determine gene orthologs using OrthoFinder v2.3.8 (Emms and Kelly 2019). To prioritize the selection of genome assemblies, the completeness of genomes was estimated using BUSCO (Manni et al. 2021), and complete or near complete genome assemblies were chosen for ortholog clustering. Of the *Alternaria* genome assemblies lacking gene annotations in GenBank, these assemblies were annotated using BRAKER2 v2.1.6 (Hoff et al. 2015). The ortholog data matrix was converted into a binary matrix, then the presence of AsCEP genes in other *Alternaria* species was calculated. To determine whether lineage-specific effector genes sit within or close to AT-rich RIP mutation hotspots, AT-rich and GC-equilibrated regions were identified using OcculterCut v1.1 (Testa et al. 2016). Any TEs within the AT-rich regions were detected using RepeatModeler v2.0.1 (Flynn et al. 2020).

Presence of AsCEP19 and AsCEP20 outside of *Alternaria*

To test whether AsCEP19 and AsCEP20 originated via HGT, the gene trees of *AsCEP19* and *AsCEP20* were compared with the species tree of *Alternaria*. Potential homologs of AsCEP19 and AsCEP20 were determined by BLASTp against UniProtKB and NCBI nr, and any BLASTp-hit with identity greater than 40% and coverage more than 70% over the query was retained.

The sequences of AsCEP19 and AsCEP20 and their homologs were aligned using MAFFT v7.453 (Standley 2013). To construct a species tree, *Alternaria* species were compared with each other and 12 fungal species from the order Pleosporales were used as the outgroup. Protein-coding genes were clustered into orthogroups using OrthoFinder v2.3.8 (Emms and Kelly 2019). In total, 1,216 single-copy orthogroups from all the fungal genomes were aligned using MAFFT, and then the multiple alignments were trimmed and concatenated into a super-matrix. The best amino acid substitute models for the alignments of AsCEP19, AsCEP20, and the concatenated super-matrix were determined using ProtTest v3.4.1 (Darriba et al. 2011). Maximum-likelihood trees were constructed using RAxML v8.2.12 (Stamatakis et al. 2005).

RNA-Seq data analysis

To determine whether homologs of AsCEP19 and AsCEP20 might play potential roles in fungal virulence, the RNA-Seq datasets were retrieved from NCBI SRA (Additional file 1: Table S3), and the expression levels of homologs were determined. Adaptor and quality trimming of raw RNA-seq datasets were performed using fastp v0.20.1 (Chen et al. 2018a, b). The trimmed reads of each sample were mapped to the corresponding fungal genomes (Additional file 1: Table S3) using HISAT2 v2.1.0 (Kim et al. 2015). Mapping results were converted to BAM format and then sorted using Samtools v1.12 (Li et al. 2009). Reads counts for each gene were calculated using the htseq-count tool in HTSeq v0.11.2 (Anders et al. 2015). Differential expression of *AsCEP19* and *AsCEP20* homologs between samples at infectious and noninfectious phases was determined using the R package DESeq2 v1.28.1 (Love et al. 2014).

Fungal isolates, plants, and culture conditions

A. solani strain HWC168 was grown on PDA plates at 25 °C in the dark, and mycelia were harvested after 8 days. To induce sporulation, strain HWC168 was grown on tomato juice agar plates in the dark at 25 °C for 8 days, and aerial hyphae were scraped off with a scalpel. The plates were subsequently exposed to UV light for 10 min and then kept in the dark at 25 °C/20 °C (12 h/12 h) for 3 days. For obtaining conidial suspensions, conidia were harvested with sterile double distilled (dd)H_2O and centrifuged at 1,970 g for 10 min, then conidia were diluted to 10^5 conidia/mL. *P. infestans* was grown on rye agar in the dark for 10 days, and mature sporangia were harvested with 2 mL of sterile ddH_2O. Sporangial suspensions were kept in the dark at 4 °C for 2 h, and then at 18 °C in the dark for 1 day to release zoospores. Potato plants (cv Favorita) were grown in a greenhouse at 24 °C with a 16/8 h light/dark cycle for 8 weeks. *N. benthamiana* plants were grown in a growth chamber at 25 °C and 50% relative humidity with 12/12 h light/dark cycles for 5 weeks. *A. thaliana* plants were grown on MS culture medium at 4 °C for 3 days, and then placed in a growth chamber at 22 °C with 16/8 h light–dark cycles. Tomato (cv Monkeymaker) and chili pepper (cv Chaotianjiao) plants were grown in a greenhouse at 24 °C with 16/8 h light–dark cycles.

Gene expression analyses using reverse transcription-quantitative polymerase chain reaction (RT-qPCR)

Expression profiles of *AsCEP19* and *AsCEP20* in strain HWC168 were determined during different stages of infection. Leaves of potato, *A. thaliana*, tomato, and chili pepper were surface-sterilized with 70% ethanol for 30 s, rinsed three times with sterile ddH_2O, dried on filter paper, and transferred to wet filter papers placed on 1% water agar in Petri dishes. Leaves were inoculated with 20 µL of *A. solani* conidial suspension or sterile ddH_2O (mock inoculation). RNA was extracted from mycelia grown in PDA and also from detached potato leaves inoculated with conidia at 12, 24, 48, and 72 hpi using EasyPure Plant RNA Kit (TransGen Beijing, China), and from detached *Arabidopsis thaliana*, tomato, and pepper leaves inoculated with conidia at 48, 72, and 96 hpi, and then treated with DNase I (TransGen). First-strand cDNA was synthesized from mRNA using TransScript First-Strand cDNA Synthesis SuperMix (TransGen) according to the manufacturer's suggestions. The gene encoding β-actin (*ACTB*) was used as an internal control. qPCR was performed on a C1000 thermal cycler equipped with a CFX96 real-time PCR detection system (Bio-Rad, CA, USA). PCR was performed with MagicSYBR Mix (CoWin BioSciences, MA, USA) and specific primers (Additional file 1: Table S7). Relative gene expression in the samples was calculated by the ddCt method (Livak and Schmittgen 2001). Two-tailed Student's *t* tests were used for comparisons between means.

Agrobacterium-mediated transient expression

To determine the phenotypic alterations induced by AsCEP19 and AsCEP20, two forms of protein, FL and ΔSP, were transiently expressed in *N. benthamiana* plants by agroinfiltration. The SP cleavage sites in AsCEP19 and AsCEP20 were predicted using SignalP. The INF1 elicitin of *P. infestans* (Kamoun et al. 1998) was used to induce plant cell death. Nucleotide sequences of $AsCEP19^{FL}$, $AsCEP19^{\Delta sp}$, $AsCEP20^{FL}$, $AsCEP20^{\Delta sp}$, and *INF1* were obtained by gene synthesis (Stargene, Wuhan, China), and all sequences were tagged with *GFP* at their C terminus. Then, nucleotide sequences fused with the *GFP*

coding sequence were cloned into the plant expression vector pCAMBIA1301. The recombinant vectors were sequenced to ensure correct insertion. *A. tumefaciens* strain EHA105 transformed with a recombinant vector was grown overnight at 28 °C in LB medium containing appropriate antibiotics. *A. tumefaciens* cells were pelleted, washed, and resuspended in infiltration buffer (10 mM $MgCl_2$, 10 mM MES, 150 μM acetosyringone). Five-week-old *N. benthamiana* leaves were infiltrated with *Agrobacterium* using a syringe without a needle. To determine whether AsCEP19 and AsCEP20 might promote the infection of pathogens, *AsCEP19* or *AsCEP20* were expressed in *N. benthamiana* leaves via agroinfiltration prior to pathogen inoculation. *Agrobacterium* carrying *GFP* and effector gene (*AsCEP19* or *AsCEP20*) plasmid constructs were injected to the left and right side of the leaf, respectively. Leaves were detached at 48 h after agroinfiltration, and subsequently inoculated with 10 μL zoospore suspension (5×10^4 zoospores/mL) of *P. infestans* and kept in Petri dishes for 5 days. The detached leaves of *N. benthamiana* were decolorized using 95% ethanol in a water bath at 100℃ for 15 min, then stained with DAB. The sizes of necrosis lesions on the leaves of *N. benthamiana* were measured and compared using paired Student's *t* test (Fig. 6c).

Subcellular localizations of AsCEP19 and AsCEP20 in *N. benthamiana* leaf cells

Determining the subcellular localization of fungal effectors in host plant cells can reveal clues about the mechanism of virulence. The *AsCEP19* and *AsCEP20* gene sequences were tagged at the C terminus with the yellow fluorescent protein-coding gene (*YFP*), and were further cloned into pCAMBIA1301 for expression in *N. benthamiana*. The recombinant vectors were sequenced to ensure correct insertion and then were transformed into *A. tumefaciens* strain GV3101. *A. tumefaciens* cells were resuspended in infiltration buffer. In addition, *A. tumefaciens* harboring a pCAMBIA1301-YFP plasmid was infiltrated into *N. benthamiana* leaves as control. The infiltrated leaves were visualized with a LEICA FCS SP8 fluorescence microscope (Leica, Germany) at 3 days post-infiltration.

Gene deletion by homologous recombination

A gene deletion mutant of *A. solani* HWC168 was generated for the contiguous region spanning the gene loci *AsCEP19*, *AsCEP20*, and the region between them. To replace the target region with *HPH* gene, a 1009 bp downstream flanking sequence of the *AsCEP19* gene (*AsCEP19RR*) and a 914 bp downstream flanking sequence of the *AsCEP20* gene (*AsCEP20RR*) were amplified with primer pairs 1920-RR-F/R and AsCEP20-RR-F1/R1, respectively (Additional file 1: Table S6). *HPH* gene fragment was amplified from the vector pEASY-HPH with primers HPH-F3/R1 (Additional file 1: Table S6). All PCR reactions were performed using Super *Pfx* DNA polymerase (CWBIO, China). Three PCR amplicons were fused in the order '*AsCEP19RR-HPH-AsCEP20RR*', and then cloned into a pUC19 vector using pEASY-Uni Seamless Cloning and Assembly Kit (TransGen, China). The fused fragment was subsequently amplified from the recombinant plasmid by PCR for transformation. Protoplasts of *A. solani* were prepared and transformed with the PCR product of the fused fragment using the polyethylene glycol (PEG4000)-mediated method (Goswami 2012). The transformants were cultured on hygromycin-resistant PDA for three generations, and the gene knockout mutants were identified by PCR using primer pairs 1920-LRHPH-F/R and 1920-RR-F-HPH/1920-RR-HPH-R (Additional file 1: Table S6), which targets the regions of *AsCEP19RR* fused with *HPH* and *AsCEP20RR* fused with *HPH*, respectively. To compare the virulence between the gene knockout mutant and wild-type strain in host potato, detached potato leaves (n = 17) were inoculated with conidial suspensions (10^5 conidia/mL) of the tested strains. The necrotic lesions were measured at 5 dpi, and paired *t*-test was performed in R v4.1.3 to determine whether there was any significant difference in virulence between the mutant and wild-type strain. Similar results were obtained from two independent experiments.

Abbreviations

AsCEPs: *Alternaria solani* candidate effector proteins; Avr: Avirulence;; CCP: *Corynespora cassiicola* strain Philippines; FL: Full length; H2H: Head-to-head; HGT: Horizontal gene transfer; LTR: Long terminal repeat; PAV: Presence-and-absence variation; RT-qPCR: Reverse transcription-quantitative polymerase chain reaction; RIP: Repeat-induced point; SP: Signal peptide; TEs: Transposable elements; YFP: Yellow fluorescent protein.

Supplementary Information

The online version contains supplementary material available at https://doi.org/10.1186/s42483-022-00135-z.

Additional file 1. Table S1. Protein-coding genes in *Alternaria solani* HWC168 and gene expressions in planta. **Table S2.** Effector genes predicted from *Alternaria solani* HWC168. **Table S3.** NCBI SRA RNA-Seq datasets used in this study. **Table S4.** Conservation of AsCEP genes in 29 *Alternaria* species. **Table S5.** The distance between candidate effector genes and nearby AT-rich region. **Table S6.** Primers used for the gene knockout and validation. **Table S7.** Primers used for the RT-qPCR analysis.

Additional file 2. Figure S1. Schematic diagram of long-range synteny between genomes of strains NL03003 and HWC168. **Figure S2.** Multiple sequence alignment of AsCEP20 and its homologs. **Figure S3.** Transient expression of *AsCEP19* and *AsCEP20* in *Nicotiana benthamiana* leaves. **Figure S4.** PCR validation of the gene pair (*AsCEP19* and *AsCEP20*) knockout mutant of *Alternaria solani* HWC168.

Acknowledgements
Not applicable.

Author contributions
JW, ZY, and JZ designed the research. JW and SX conducted the bioinformatics analyses. SX, LZ, YP, DMZ, DZ, and QL collected the data. SX, JW, and LZ performed the experiments. SX and JW wrote the manuscript. All authors read and approved the final manuscript.

Funding
This research work was supported by the National Natural Science Foundation of China (Grant No. 32070143), and also funded by Hebei Agricultural University (Grant No. YJ2020015) and State Key Laboratory of North China Crop Improvement and Regulation, NCCIR (Grant No. NCCIR2020RC-8), and Hebei key Research and Development Program (Grant No. 21326320D).

Availability of data and materials
Data sets used or analyzed during the current study are publicly available. The genome sequence of *A. solani* HWC168 and the RNA-Seq dataset have been deposited at the National Center for Biotechnology Information under the the project number PRJNA263761 and PRJNA574559, respectively.

Declarations

Ethics approval and consent to participate
Not applicable.

Consent for publication
Not applicable.

Competing interests
The authors declare that they have no competing interests.

Author details
[1]College of Plant Protection, Hebei Agricultural University, Baoding 071001, Hebei, China. [2]State Key Laboratory of North China Crop Improvement and Regulation, Baoding 071001, Hebei, China.

Received: 14 April 2022 Accepted: 20 July 2022
Published online: 08 August 2022

References

Adhikari TB, Bai J, Meinhardt SW, Gurung S, Myrfield M, Patel J, et al. Tsn1-mediated host responses to ToxA from *Pyrenophora tritici-repentis*. Mol Plant Microbe Interact. 2009;22(9):1056–68. https://doi.org/10.1094/MPMI-22-9-1056.

Adhikari P, Oh Y, Panthee DR. Current status of early blight resistance in tomato: an update. Int J Mol Sci. 2017;18(10):2019. https://doi.org/10.3390/ijms18102019.

Anders S, Pyl PT, Huber W. HTSeq—a Python framework to work with high-throughput sequencing data. Bioinformatics. 2015;31(2):166–9. https://doi.org/10.1093/bioinformatics/btu638.

Batanghari JW, Deepe GS Jr, Di Cera E, Goldman WE. *Histoplasma* acquisition of calcium and expression of *CBP1* during intracellular parasitism. Mol Microbiol. 1998;27(3):531–9. https://doi.org/10.1046/j.1365-2958.1998.00697.x.

Beck MR, DeKoster GT, Hambly DM, Gross ML, Cistola DP, Goldman WE. Structural features responsible for the biological stability of *Histoplasma*'s virulence factor CBP. Biochemistry. 2008;47(15):4427–38. https://doi.org/10.1021/bi701495v.

Borah N, Albarouki E, Schirawski J. Comparative methods for molecular determination of host-specificity factors in plant-pathogenic fungi. Int J Mol Sci. 2018;19(3):863. https://doi.org/10.3390/ijms19030863.

Chen Y, Yu H, Li Y, Li Y. Sorting out inherent features of head-to-head gene pairs by evolutionary conservation. BMC Bioinformatics. 2010;11(Suppl 11):S16. https://doi.org/10.1186/1471-2105-11-S11-S16.

Chen J, Liu C, Gui Y, Si K, Zhang D, Wang J, et al. Comparative genomics reveals cotton-specific virulence factors in flexible genomic regions in *Verticillium dahliae* and evidence of horizontal gene transfer from *Fusarium*. New Phytol. 2018a;217(2):756–70. https://doi.org/10.1111/nph.14861.

Chen S, Zhou Y, Chen Y, Gu J. Fastp: an ultra-fast all-in-one FASTQ preprocessor. Bioinformatics. 2018b;34(17):i884–90. https://doi.org/10.1093/bioinformatics/bty560.

Dalio RJD, Herlihy J, Oliveira TS, Mcdowell JM, Machado MAA. Effector biology in focus: a primer for computational prediction and functional characterization. Mol Plant Microbe Interact. 2018;31(1):22–33. https://doi.org/10.1094/MPMI-07-17-0174-FI.

Dang HX, Pryor B, Peever T, Lawrence CB. The *Alternaria* genomes database: a comprehensive resource for a fungal genus comprised of saprophytes, plant pathogens, and allergenic species. BMC Genomics. 2015;16(1):239. https://doi.org/10.1186/s12864-015-1430-7.

Darriba D, Taboada GL, Doallo R, Posada D. ProtTest 3: fast selection of best-fit models of protein evolution. Bioinformatics. 2011;27(8):1164–5. https://doi.org/10.1093/bioinformatics/btr088.

de Torres ZM, Littlejohn G, Jayaraman S, Studholme D, Bailey T, Lawson T, et al. Chloroplasts play a central role in plant defence and are targeted by pathogen effectors. Nat Plants. 2015;1(6):1507. https://doi.org/10.1038/nplants.2015.74.

de Vries S, Stukenbrock EH, Rose LE. Rapid evolution in plant-microbe interactions-an evolutionary genomics perspective. New Phytol. 2020;226(5):1256–62. https://doi.org/10.1111/nph.16458.

Dita MA, Brommonschenkel SH, Matsuoka K, Mizubuti ESG. Histopathological study of the *Alternaria solani* infection process in potato cultivars with different levels of early blight resistance. J Phytopathol. 2007;155(7–8):462–9. https://doi.org/10.1111/j.1439-0434.2007.01258.x.

Dong S, Ma W. How to win a tug-of-war: the adaptive evolution of *Phytophthora* effectors. Curr Opin Plant Biol. 2021;62: 102027. https://doi.org/10.1016/j.pbi.2021.102027.

Emms D, Kelly S. OrthoFinder: phylogenetic orthology inference for comparative genomics. Genome Biol. 2019;20(1):238. https://doi.org/10.1186/s13059-019-1832-y.

Flynn JM, Hubley R, Goubert C, Rosen J, Clark AG, Feschotte C, et al. RepeatModeler2 for automated genomic discovery of transposable element families. Proc Natl Acad Sci USA. 2020;117(17):9451–7. https://doi.org/10.1073/pnas.1921046117.

Fouché S, Plissonneau C, Croll D. The birth and death of effectors in rapidly evolving filamentous pathogen genomes. Curr Opin Microbiol. 2018;46:34–42. https://doi.org/10.1016/j.mib.2018.01.020.

Frantzeskakis L, Di Pietro A, Rep M, Schirawski J, Wu CH, Panstruga R. Rapid evolution in plant–microbe interactions–a molecular genomics perspective. New Phytol. 2020;225(3):1134–42. https://doi.org/10.1111/nph.15966.

Friesen TL, Stukenbrock EH, Liu Z, Meinhardt S, Ling H, Faris JD, et al. Emergence of a new disease as a result of interspecific virulence gene transfer. Nat Genet. 2006;38(8):953–6. https://doi.org/10.1038/ng1839.

Gannibal PB, Orina AS, Mironenko NV, Levitin MM. Differentiation of the closely related species, Alternaria solani and A. tomatophila, by molecular and morphological features and aggressiveness. Eur J Plant Pathol. 2014;139(3):609–23. https://doi.org/10.1007/s10658-014-0417-6.

Gilmore SA, Voorhies M, Gebhart D, Sil A. Genome-wide reprogramming of transcript architecture by temperature specifies the developmental states of the human pathogen *Histoplasma*. PLoS Genet. 2015;11(7):e1005395. https://doi.org/10.1371/journal.pgen.1005395.

Gíslason MH, Nielsen H, Armenteros JJA, Johansen AR. Prediction of GPI-anchored proteins with pointer neural networks. Curr Res Biotechnol. 2021;3:6–13. https://doi.org/10.1101/838680.

Goswami RS. Targeted gene replacement in fungi using a split-marker approach. In: Bolton M, Thomma B, editors. Plant Fungal Pathogens. Methods in Molecular Biology, vol. 835. Humana Totowa, NJ: Humana Press; 2012. https://doi.org/10.1007/978-1-61779-501-5_16.

Grabherr MG, Haas BJ, Yassour M, Levin JZ, Thompson DA, Amit I, et al. Full-length transcriptome assembly from RNA-Seq data without a reference genome. Nat Biotechnol. 2011;29(7):644–52. https://doi.org/10.1038/nbt.1883.

Haas BJ, Delcher AL, Mount SM, Wortman JR, Smith RK Jr, Hannick LI, et al. Improving the *Arabidopsis* genome annotation using maximal transcript alignment assemblies. Nucleic Acids Res. 2003;31(19):5654–66. https://doi.org/10.1093/nar/gkg770.

Haas BJ, Salzberg SL, Zhu W, Pertea M, Allen JE, Orvis J, et al. Automated eukaryotic gene structure annotation using evidence modeler and the program to assemble spliced alignments. Genome Biol. 2008;9(1):1–22. https://doi.org/10.1186/gb-2008-9-1-r7.

Hoff KJ, Lange S, Lomsadze A, Borodovsky M, Stanke M. BRAKER1: unsupervised RNA-Seq-based genome annotation with GeneMark-ET and AUGUSTUS. Bioinformatics. 2015;32(5):767–9. https://doi.org/10.1093/bioinformatics/btv661.

Horton P, Park KJ, Obayashi T, Fujita N, Harada H, et al. WoLF PSORT: protein localization predictor. Nucleic Acids Res. 2007;35(Suppl 2):W585–7. https://doi.org/10.1093/nar/gkm259.

Kamoun S, van West P, Vleeshouwers VG, de Groot KE, Govers F. Resistance of *Nicotiana benthamiana* to *Phytophthora infestans* is mediated by the recognition of the elicitor protein INF1. Plant Cell. 1998;10(9):1413–26. https://doi.org/10.1105/tpc.10.9.1413.

Kettles GJ, Bayon C, Sparks CA, Canning G, Kanyuka K, Rudd JJ. Characterization of an antimicrobial and phytotoxic ribonuclease secreted by the fungal wheat pathogen *Zymoseptoria tritici*. New Phytol. 2018;217(1):320–31. https://doi.org/10.1111/nph.14786.

Kim D, Langmead B, Salzberg SL. HISAT: a fast spliced aligner with low memory requirements. Nat Methods. 2015;12(4):357–60. https://doi.org/10.1038/nmeth.3317.

Krogh A, Larsson B, von Heijne G, Sonnhammer EL. Predicting transmembrane protein topology with a hidden Markov model: application to complete genomes. J Mol Biol. 2001;305(3):567–80. https://doi.org/10.1006/jmbi.2000.4315.

Li H, Handsaker B, Wysoker A, Fennell T, Ruan J, Homer N, et al. The sequence alignment/map (SAM) format and SAMtools. Bioinformatics. 2009;25(16):2078–9. https://doi.org/10.1093/bioinformatics/btp352.

Livak KJ, Schmittgen TD. Analysis of relative gene expression data using real-time quantitative PCR and the $2^{-\Delta\Delta C}{}_{T}$ method. Methods. 2001;25(4):402–8. https://doi.org/10.1006/meth.2001.1262.

Lo Presti L, Lanver D, Schweizer G, Tanaka S, Liang L, Tollot M, et al. Fungal effectors and plant susceptibility. Annu Rev Plant Biol. 2015;66:513–45. https://doi.org/10.1146/annurev-arplant-043014-114623.

Lopez D, Ribeiro S, Label P, Fumanal B, Venisse JS, Kohler A, et al. Genome-wide analysis of *Corynespora cassiicola* leaf fall disease putative effectors. Front Microbiol. 2018;9:276. https://doi.org/10.3389/fmicb.2018.00276.

Love MI, Huber W, Anders S. Moderated estimation of fold change and dispersion for RNA-seq data with DESeq2. Genome Biol. 2014;15(12):550. https://doi.org/10.1186/s13059-014-0550-8.

Ma LJ, van der Does HC, Borkovich KA, Coleman JJ, Daboussi MJ, Di Pietro A, et al. Comparative genomics reveals mobile pathogenicity chromosomes in *Fusarium*. Nature. 2010;464(7287):367–73. https://doi.org/10.1038/nature08850.

Manni M, Berkeley MR, Seppey M, Simão FA, Zdobnov EM. BUSCO update: novel and streamlined workflows along with broader and deeper phylogenetic coverage for scoring of eukaryotic, prokaryotic, and viral genomes. Mol Biol Evol. 2021;38(10):4647–54. https://doi.org/10.1093/molbev/msab199.

McDonald MC, Taranto AP, Hill E, Schwessinger B, Liu Z, Simpfendorfer S, et al. Transposon-mediated horizontal transfer of the host-specific virulence protein toxa between three fungal wheat pathogens. mBio. 2019;10(5):e01515-19. https://doi.org/10.1128/mBio.01515-19.

Meena M, Gupta SK, Swapnil P, Zehra A, Dubey MK, Upadhyay RS. *Alternaria* toxins: potential virulence factors and genes related to pathogenesis. Front Microbiol. 2017;8:1451. https://doi.org/10.3389/fmicb.2017.01451.

Ozkilinc H, Rotondo F, Pryor BM, Peever TL. Contrasting species boundaries between sections *Alternaria* and *Porri* of the genus *Alternaria*. Plant Pathol. 2017;67(2):303–14. https://doi.org/10.1111/ppa.12749.

Rajarammohan S, Paritosh K, Pental D, Kaur J. Comparative genomics of *Alternaria* species provides insights into the pathogenic lifestyle of *Alternaria brassicae*-a pathogen of the *Brassicaceae* family. BMC Genomics. 2019;20(1):1036. https://doi.org/10.1186/s12864-019-6414-6.

Reinhardt D, Roux C, Corradi N, Di Pietro A. Lineage-specific genes and cryptic sex: parallels and differences between arbuscular mycorrhizal fungi and fungal pathogens. Trends Plant Sci. 2021;26(2):111–23. https://doi.org/10.1016/j.tplants.2020.09.006.

Sánchez-Vallet A, Fouché S, Fudal I, Hartmann FE, Soyer JL, Tellier A, et al. The genome biology of effector gene evolution in filamentous plant pathogens. Annu Rev Phytopathol. 2018;56:21–40. https://doi.org/10.1146/annurev-phyto-080516-035303.

Sebghati TS, Engle JT, Goldman WE. Intracellular parasitism by *Histoplasma capsulatum*: fungal virulence and calcium dependence. Science. 2000;290(5495):1368–72. https://doi.org/10.1126/science.290.5495.1368.

Sperschneider J, Dodds PN. EffectorP 3.0: prediction of apoplastic and cytoplasmic effectors in fungi and oomycetes. Mol Plant Microbe Interact. 2022;35(2):146–56. https://doi.org/10.1094/MPMI-08-21-0201-R.

Stamatakis A, Ludwig T, Meier H. RAxML-III: a fast program for maximum likelihood-based inference of large phylogenetic trees. Bioinformatics. 2005;2(4):456–63. https://doi.org/10.1093/bioinformatics/bti191.

Standley K, Standley DM. MAFFT multiple sequence alignment software version 7: improvements in performance and usability. Mol Biol Evol. 2013;30(4):772–80. https://doi.org/10.1093/molbev/mst010.

Testa AC, Oliver RP, Hane JK. OcculterCut: a comprehensive survey of AT-rich regions in fungal genomes. Genome Biol Evol. 2016;8(6):2044–64. https://doi.org/10.1093/gbe/evw121.

Teufel F, Almagro Armenteros JJ, Johansen AR, Gíslason MH, Pihl SI, Tsirigos KD, et al. SignalP 6.0 predicts all five types of signal peptides using protein language models. Nat Biotechnol. 2022. https://doi.org/10.1038/s41587-021-01156-3.

Torres DE, Oggenfuss U, Croll D, Seidl MF. Genome evolution in fungal plant pathogens: looking beyond the two-speed genome model. Fungal Biol Rev. 2020;34(3):136–43. https://doi.org/10.1016/j.fbr.2020.07.001.

Tsuge T, Harimoto Y, Akimitsu K, Ohtani K, Kodama M, Akagi Y, et al. Host-selective toxins produced by the plant pathogenic fungus *Alternaria alternata*. FEMS Microbiol Rev. 2013;37(1):44–66. https://doi.org/10.1111/j.1574-6976.2012.00350.x.

Wang Y, Tang H, Debarry JD, Tan X, Li J, Wang X, et al. *MCScanX*: a toolkit for detection and evolutionary analysis of gene synteny and collinearity. Nucleic Acids Res. 2012;40(7): e49. https://doi.org/10.1093/nar/gkr1293.

Wang M, Fu H, Shen XX, Ruan R, Rokas A, Li H. Genomic features and evolution of the conditionally dispensable chromosome in the tangerine pathotype of *Alternaria alternata*. Mol Plant Pathol. 2019;20(10):1425–38. https://doi.org/10.1111/mpp.12848.

Wang D, Tian L, Zhang DD, Song J, Song SS, Yin CM, et al. Functional analyses of small secreted cysteine-rich proteins identified candidate effectors in *Verticillium dahliae*. Mol Plant Pathol. 2020;21(5):667–85. https://doi.org/10.1111/mpp.12921.

Wei M, Wang A, Liu Y, Ma L, Niu X, Zheng A. Identification of the novel effector RsIA_NP8 in *Rhizoctonia solani* AG1 IA that induces cell death and triggers defense responses in non-host plants. Front Microbiol. 2020;11:1115. https://doi.org/10.3389/fmicb.2020.01115.

Wolters PJ, Faino L, van den Bosch TBM, Evenhuis B, Visser RGF, Seidl MF, et al. Gapless genome assembly of the potato and tomato early blight pathogen *Alternaria solani*. Mol Plant-Microbe Interact. 2018;31(7):692–4. https://doi.org/10.1094/MPMI-12-17-0309-A.

Woudenberg JH, Truter M, Groenewald JZ, Crous PW. Large-spored *Alternaria* pathogens in section *Porri* disentangled. Stud Mycol. 2014;79(1):1–47. https://doi.org/10.1016/j.simyco.2014.07.003.

Yang B, Wang Y, Tian M, Dai K, Zheng W, Liu Z, et al. Fg12 ribonuclease secretion contributes to *Fusarium graminearum* virulence and induces plant cell death. J Integr Plant Biol. 2021;63(2):365–77. https://doi.org/10.1111/jipb.12997.

Zhang D, He JY, Haddadi P, Zhu JH, Yang ZH, Ma L. Genome sequence of the potato pathogenic fungus *Alternaria solani* HWC-168 reveals clues for its conidiation and virulence. BMC Microbiol. 2018;18(1):176. https://doi.org/10.1186/s12866-018-1324-3.

Zhang Y, Yang H, Turra D, Zhou S, Ayhan DH, Delulio GA, et al. The genome of opportunistic fungal pathogen *Fusarium oxysporum* carries a unique set of lineage-specific chromosomes. Commun Biol. 2020;3(1):50. https://doi.org/10.1038/s42003-020-0770-2.